

## Abstract

Angle-dependent magnetoresistance (ADM) has been used to identify two distinct inelastic scattering channels in the high temperature copper-oxide superconductor (HTSC)  $Tl_2Ba_2Ca_0Cu_1O_{6+\delta}$  (Tl2201). One of these channels is found to be isotropic around the Fermi Surface with a magnitude proportional to  $T^2$ . The other channel is found to be highly anisotropic with the same four fold symmetry as the superconducting gap and a magnitude that grows linearly with temperature. Significantly, this form of scattering rate can account for the temperature dependence of both the in-plane resistivity and Hall effect at a doping of  $p \approx 0.24$  ( $T_c \approx 15K$ ). At fixed temperature we identify an approximately linear correlation between a normal state property (the magnitude of the anisotropic scattering) and  $T_c$  which, intriguingly extrapolates to zero at the doping level where superconductivity vanishes.

## Introduction

Understanding the properties of their normal state is generally regarded as a key step in understanding HTSC. In overdoped samples the temperature dependence of the resistivity generally fits to  $A+BT+CT^2$  with the  $T^2$  term beginning to dominate as doping increases but  $R_{Hl}$  is  $T$  dependent and varies in a non-symmetric way [1]. One way of interpreting this is to consider two decoupled scattering rates with different  $T$  dependences - the resistivity depending on  $1/\tau_{\parallel}$  and  $\cot\theta_{\parallel}$  depending on  $1/\tau_{\perp}$  with  $R_{Hl}$  sensitive to  $\tau_{\parallel}/\tau_{\perp}$ . In this work we uncover two scattering rates in Tl2201 (one of which is anisotropic) with distinct temperature dependences and use this to accurately simulate  $\rho_{ab}$  and  $R_{Hl}$ .

## Tl2201

Overdoped Tl2201 is one of the cleanest copper-oxide based superconductors with a low residual resistivity and low upper critical field. Its  $T_c$  can be adjusted from optimally doped ( $T_c \approx 90K$ ) by changing the hole concentration. The band-structure in Fig. 1 shows a large hole pocket around the X point of the Brillouin zone and a small electron pocket around the  $\Gamma$  point (which is not seen by AMRO or ARPES [2] studies, but is predicted to rise above  $\epsilon_F$  when doping is accounted for in the bandstructure calculations).

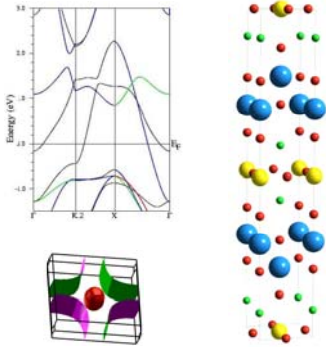


Fig. 1 – Top: Undoped Tl2201 bandstructure (Wien2K). Bottom: Tl2201 Fermi surface from Wien2K. Right: Undoped Tl2201 crystal structure Blue=Ti, Green=Ba, Yellow=Cu, Red=O.

## Experiment

Single crystals of Tl2201 were fabricated using a self-flux method in alumina crucibles. As grown crystals are overdoped and their  $T_c$  was set by annealing in oxygen or argon. Electrical contacts were attached using Dupont 6838 silver paste. Measurements were carried out on a number of crystals ( $\approx 300\mu m \times 150\mu m \times 20\mu m$ ) with  $T_c \approx 15K$  in the 45T hybrid magnet at NHMFL, Tallahassee, Florida using a two axis rotator probe. Angle dependent magnetoresistance data was taken at constant temperature while sweeping the angle  $\theta$  and then repeated at various different temperatures and angles  $\phi$ .

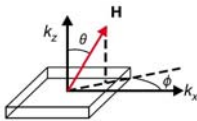


Fig. 2 – ADMR sample geometry.

In a large magnetic field electrons are driven around the Fermi surface in orbits in the plane perpendicular to the applied field. Maxima in the interplane resistivity occur when the interplane velocity averaged around the Fermi surface is zero. Clearly for a simple cylinder no effect would be seen. Contrastingly, for a barrel shaped Fermi surface Yamaji [3] showed that oscillations (AMRO) occur in the resistivity at angles given by  $\cot\theta \tan\theta = \pi(n-1/4)$ . In Tl2201 at 45T and at low temperature,  $\omega_c \tau$  is not large enough to see Yamaji oscillations, but our data and analysis show that an angle dependent resistivity due to the Fermi surface topology and anisotropic scattering is still clearly visible.

## Analysis

We have shown previously that the Shockley-Chambers tube integral form of the Boltzmann transport equation can be used along with a 3D dispersion relation to accurately fit Tl2201 AMRO [4]. Fitting to the parameters  $k_{00}$ ,  $k_{60}/k_{21}$  and  $k_{101}/k_{21}$  along with  $\omega_c \tau$  is sufficient to fit the data at 4.2K.

$$k_{\phi} = k_{00} + k_{60} \cos 4\phi + k_{21} \cos\left(\frac{c k_z}{2}\right) \left[ \sin 2\phi + \frac{k_{101}}{k_{21}} \sin 6\phi + \frac{k_{101}}{k_{21}} \sin 10\phi \right]$$

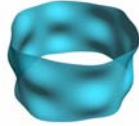


Fig. 3 - Fermi surface suggested by data. Warping has been enhanced for clarity.

However, as temperature increases the fits worsen. We find that to fit the data (see Fig. 3) we need to relax the constraint that  $\omega_c \tau$  remains isotropic in the basal plane. We introduce anisotropy in both the in-plane velocity  $v_{\parallel}(\phi) = v_F^2(1 + \beta \cos 4\phi)$  and scattering rate  $1/\tau_{\perp}(\phi) = (1 + \alpha \cos 4\phi)/\tau^2$  [5] in the simplest form compatible with the bct crystal symmetry. The  $\phi$  dependent scattering rate can be re-expressed as the sum of an isotropic component and an anisotropic component with the same symmetry as the superconducting d-wave gap.

$$\frac{1}{\omega_c^2 \tau(\phi)} = \frac{(1 + \alpha \cos 4\phi)}{\omega_c^2 \tau^2} = \frac{(1 - \alpha)}{\omega_c^2 \tau^2} + \frac{2\alpha \cos^2 2\phi}{\omega_c^2 \tau^2}$$

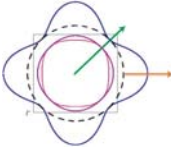


Fig. 4 – Black dashed line – isotropic component of  $\tau$ . Blue line – anisotropic component of  $\tau$ . Red – 2D projection of the Fermi surface. Purple line – schematic representation of the d-wave superconducting gap.

As there is no experimental evidence to suggest significant changes in the Fermi surface topography with temperature we fix the Fermi surface parameters ( $k_{00}$ ,  $k_{60}/k_{21}$  and  $k_{101}/k_{21}$ ) and  $\beta$  to their 4.2K values and allow only  $\alpha$  and  $\omega_c^2 \tau^2$  to vary with temperature.

## Data

Previous work [5] included data on one sample for only one azimuthal angle ( $\phi$ ) covering a temperature range up to 50K. Recently we have extended this work to cover 3 further samples - each over 5 azimuthal angles and at temperatures up to 90K. Data for one sample is presented in Fig. 5 Left along with a corresponding fit in Fig. 5 Right. It is notable that the data has features visible up to 90K and that the fits are also robust to 90K.

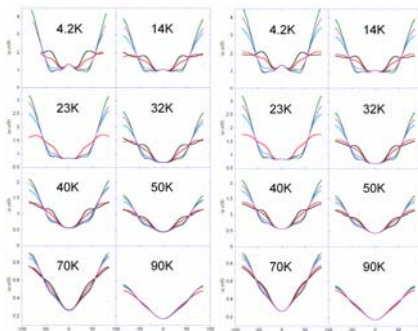


Fig. 5 - Left: ADMR experimental data for five different  $\phi$ . Right: Corresponding simulation of data with all Fermi surface parameters fixed at their 4.2K values. Black  $\phi=0^\circ$  (to Cu-O-Cu bond), red  $\phi=19^\circ$ , blue  $\phi=32^\circ$ , green  $\phi=45^\circ$  and purple  $\phi=55^\circ$ .

## Temperature

The isotropic component increases as  $T^2$  and the anisotropic component rises linearly with temperature from approximately zero at 0K. Fig. 6 shows that this "lifetime separation" is robust up to 90K!

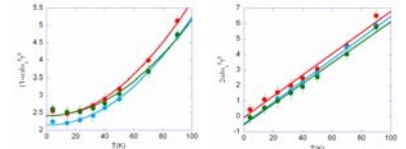


Fig. 6 – Left: Isotropic component of  $1/\tau_{\perp}(\phi)$  with  $A+BT^2$  fit. Right anisotropic component of  $1/\tau_{\perp}(\phi)$  with  $C+DT$  fit. Data for 4 samples with  $T_c = 15K \pm 3K$ .

## $\rho_{ab}$ & $R_H$

Using the Jones-Zener expansion of the linearised Boltzmann transport equation and parameters derived from our ADMR fits the in-plane resistivity with its strong T-linear term at low T can be quantitatively fitted. Along with the simulation of the strongly T dependent Hall coefficient it provides powerful evidence that the T dependence of both can be explained in an anisotropic scattering picture.

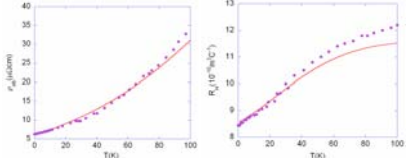


Fig. 7 – Left: In-plane resistivity. Right: Hall coefficient. Data for same 4 samples as in Fig. 6. Purple spots – data extracted from [1], coloured lines – fits.

## Doping

From AMRO data taken at 40K on crystals with a range of  $T_c$ s we find that the magnitude of the isotropic component remains constant with  $T_c$ . By contrast the magnitude of the anisotropic component scales linearly with  $T_c$  [6]. Intriguingly this extrapolates to zero at the doping where superconductivity vanishes.

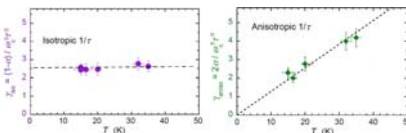


Fig. 8 – Left: Doping dependence of the isotropic component. Right: Doping dependence of the anisotropic component of  $1/\tau_{\perp}(\phi)$  at 40K.

Notably, in non-superconducting cuprates, the in-plane resistivity varies as  $T^2$  at low temperatures with no evidence of a T-linear term [7]. This implies that the development of superconductivity (from the overdoped side) is closely correlated with the appearance of the T-linear resistivity and an anisotropic scattering rate.

## Summary

The isotropic scattering component (proportional to  $T^2$ ) is not dependent on doping. The anisotropic part is proportional to T and decreases linearly as doping is increased – disappearing at the doping level where superconductivity vanishes. The challenge now is to identify the origin of the anisotropic scattering and to confirm the linearity of the anisotropic scattering rate versus doping graph over a wider doping and temperature range.

## References

- [1] A. P. Mackenzie, PRB 53 5848 (1996)
- [2] M. Pflue, PRL 95 077001 (2005)
- [3] K. Yamaji, JPSJ 58 1520 (1989)
- [4] N. Hussey, Nature 425 814 (2003)
- [5] M. Abdel-Jawad, Nat. Phys. 2 821 (2006)
- [6] M. Abdel-Jawad, submitted to PRL (2007)
- [7] S. Nakamae PRB 68 100502 (2003)